Published in final edited form as:
J Invest Dermatol. 2009 March ; 129(3): 657–670. doi:10.1038/jid.2008.298.

Auf1/*Hnrnpd*-Deficient Mice Develop Pruritic Inflammatory Skin Disease

Navid Sadri[1] and **Robert J. Schneider**[1]

[1]Department of Microbiology, New York University School of Medicine, New York, New York, USA

Abstract

Mice lacking heterogenous nuclear ribonuclear protein D (*Hnrnpd*), also known as Auf1, a regulator of inflammatory cytokine mRNA stability, develop chronic dermatitis with age that is characterized by pruritis and excoriations. Histological analysis showed marked epidermal acanthosis and spongiosis, neovascularization, and elevated number of inflammatory cells, including T cells, macrophages, neutrophils, mast cells, and eosinophils. *Hnrnpd*-deficient (*Hnrnpd*^{tm1Rjsc}) mice with dermatitis display elevated serum IgE levels. Lesions in *Hnrnpd*^{tm1Rjsc} mice were associated with a shift towards a Th_2 immune environment. Evaluation of T-cell-mediated skin inflammation by assaying contact hypersensitivity indicated an increased response in *Hnrnpd*^{tm1Rjsc} mice. T cells and macrophages from *Hnrnpd*^{tm1Rjsc} mice demonstrate a number of abnormalities associated with dermatitis, including increased IL2, tumor-necrosis factor-α (TNFα), and IL1β production. Finally, many features of spontaneous dermatitis could be recapitulated in experimentally induced lesions by subcutaneous injection of CCL27 and TNF in unaffected *Hnrnpd*^{tm1Rjsc} mice. Collectively, these data highlight the importance of HNRNPD and proper regulation of mRNA stability in the intricate processes of leukocyte recruitment and inflammatory activation within the skin.

INTRODUCTION

Atopic dermatitis (AD) is a common chronic pruritic inflammatory disease that typically occurs in early childhood, but it can persist into or present in adulthood (Leung *et al*., 2004; Boguniewicz *et al*., 2006). AD is often associated with subsequent development of other atopic conditions, such as asthma and allergic rhinoconjunctivitis (Leung *et al*., 2004; Boguniewicz *et al*., 2006). Both genetic and environmental factors are important in the development of the disease (Leung *et al*., 2004; Hoffjan and Epplen, 2005). The etiology of the disease is unknown, although 70–80% of AD patients have elevated serum IgE levels suggesting an association with an allergic response (Leung *et al*., 2004). Treatment of AD is largely limited to antiinflammatory drugs, such as corticosteroids, that show transient effect

Correspondence: Dr Robert J. Schneider, Department of Microbiology, New York University School of Medicine, 550 First Avenue, New York, New York 10003, USA. Rober.Schneider@nyumc.org.

CONFLICTS OF INTEREST

The authors state no conflict of interest.

on symptoms. A better understanding of the mechanisms underlying the etiology and chronic nature of the disease is critical for development of more effect therapeutic strategies.

The pathophysiology of AD involves complex interactions among the host's environment, the skin's barrier functions, as well as systemic and local immunological responses orchestrated by inflammatory cytokines and chemokines (Leung *et al*., 2004; Avgerinou *et al*., 2008). A large number of these inflammatory cytokines, including IL1, IL4, IL5, IL10, IL12, IL13, IL17, IFN-γ, and tumor-necrosis factor-α (TNFα), are encoded by mRNAs that contain AU-rich elements (ARE) in their 3′-untranslated region (Halees *et al*., 2008). The ARE through the interaction with ARE-binding proteins governs the stability and translation of its corresponding mRNA (Barreau *et al*., 2005). Heterogeneous nuclear riboncleoprotein D (HNRNPD), commonly referred to as ARE/poly-(U) binding degradation factor 1 (Auf1), is an ARE-binding protein that is important in the regulation of ARE-mRNA stability (Barreau *et al*., 2005; Lu *et al*., 2006). We have previously shown that disruption of *Hnrnpd* gene expression in an engineered knockout mouse model, *Hnrnpd* ^{tm1Rjsc}, sensitizes mice to endotoxic shock and increased mortality as a result of an increased and prolonged TNF and IL1β-mediated proinflammatory response (Lu *et al*., 2006). This study demonstrates the physiological role of HNRNPD in regulating the expression of ARE-containing mRNAs and highlights the consequence on immunological responses when this regulation is lost. HNRNPD is not only highly expressed in immune cells (Lu and Schneider, 2004) but also shows strong staining in the skin (Figure S1b). Thus we hypothesized that in response to environmental triggers, the activation and inability to attenuate inflammatory pathways would result in inflammatory dermatoses in *Hnrnpd* ^{tm1Rjsc} mice.

Here we show that *Hnrnpd*^{tm1Rjsc} mice develop chronic pruritic eczematous skin dermatitis that resembles some clinical and histological features of human AD. *Hnrnpd* ^{tm1Rjsc} mice exhibit enhanced contact hypersensitivity (CHS) characterized by marked increase in T lymphocytes and macrophages infiltration, as well as a significant increase in proinflammatory cytokines. Finally, recruitment of T cells in a proinflammatory environment, created by subcutaneous injection of TNF and CCL27, resulted in eczematous lesions in *Hnrnpd* ^{tm1Rjsc} mice but not in wild-type littermates. These lesions share many features of spontaneous dermatitis seen in *Hnrnpd* ^{tm1Rjsc} mice, suggesting an important role of T-cells concomitant with a proinflammatory environment in the etiology of these lesions in mice lacking *Hnrnpd*.

RESULTS

Hnrnpd^{tm1Rjsc} mice develop spontaneous inflammatory skin lesions

Hnrnpd ^{tm1Rjsc} mice exhibit signs of cutaneous periocular changes around 2–3 months of age that develop into pruritic erythematous ulcerative lesions primarily located on the face, rostrum, ear, and neck. The majority of lesions invariably begin with palpebral swelling (Figure 1b and c). The initial blepharitis is later accompanied with periocular edema that often results in palpebral closure, as well as serous exudates and crust formation (Figure 1d). Lesions invariably progress below the eye (Figure 1e) and continue to spread to the neck in severely affected mice (Figure 1f). This progression is believed to be a result of excoriation, as affected mice scratch intensely at sites of lesions. Chronic lesions are characterized by

lichenification of the skin with scaly white appearance (Figure 1g and h). About 25% of affected animals present with crust formation and ulcers on the pinna, external ear canal (Figure 1i), or dorsum rather than with periocular lesions.

Blepharitis and dermatitis are restricted to homozygote *Hnrnpd* ^{tm1Rjsc} mice, as heterozygous and wild-type littermates are free of disease. To facilitate the description of the phenotype, a “skin lesion” was categorized as involvement of tissue outside of palpebral involvement upon gross examination (refer to Figure 1e–i). A lesion includes both contiguous spread to surrounding tissue from periocular involvement and dermatitis in locations distant from or without periocular involvement. Age of onset and incidence of skin lesions is shown in Figure 1j. 129S6/SvEvTac (129S6)-*Hnrnpd* ^{tm1Rjsc} mice show earlier onset and higher incidence of skin lesions than B6;129S6-*Hnrnpd* ^{tm1Rjsc} mice (Figure 1j). However no differences were observed in the gross pathology or histological analysis of lesions from these two backgrounds. The sex of the animals had no impact on the onset, incidence, or severity of disease. Owing to the size of our 129S6-*Hnrnpd* ^{tm1Rjsc} mouse colony, studies and analysis described in this report were performed in B6;129S6-*Hnrnpd* ^{tm1Rjsc} mice and wild-type sex-match littermates were used as controls, unless otherwise stated. Preliminary studies performed in 129S6-*Hnrnpd* ^{tm1Rjsc} mice mirror the results seen in CHS experiments and in characterization of inflammatory cells carried out in B6;129S6-*Hnrnpd* ^{tm1Rjsc} mice.

Two independently bred populations of *Hnrnpd* ^{tm1Rjsc} mice in separate animal facilities maintained by clean animal husbandry protocols developed spontaneous lesions at similar frequencies and rates. In approximately 15% of cases, bacterial pyoderma containing staphylococcal colonies were found on denuded surfaces of skin lesions by histological examination. However, bacterial colonies were not found in the dermis or in other organs. Histological examination may underestimate the presence of staphylococcus in skin lesions as bacterial cultures of chronic lesions in three *Hnrnpd*1^{tm1Rjsc} mice tested were all positive for *Staphylococcus aureus*. Affected *Hnrnpd* ^{tm1Rjsc} mice were unresponsive to topical and oral antibiotics, although lesions showed improvement in response to subcutaneous and topical corticosteroid treatment. Improvement was not permanent, as lesion severity returned with cessation of immunosuppressive treatment.

Histological examination of lesions

Histological examination of normal skin from *Hnrnpd* ^{tm1Rjsc} mice with lesions revealed normal epidermal thickness and a trace of mononuclear cells in the dermis (Figure 2a). However, histological analysis of skin neighboring lesions showed a large dermal infiltration of neutrophils, mononuclear cells, and a few eosinophils with minimal epidermal morphological changes (Figure 2b and c), suggesting leukocyte infiltration precedes epidermal proliferation in disease progression. Histological examination of chronic skin lesions demonstrates marked acanthosis of the epidermis with spongiosis, hyperkeratosis with focal areas of parakeratosis, and prominent dermal and epidermal infiltration of leukocytes (Figure 2d–g). Phosphorylation of the signal transducer and activator of transcription 3 (Stat3) at Tyr705 (PY-Stat3) is seen in psoriatic lesions (Sano *et al*., 2005) and animal models of induced epidermal hyperplasia (Chan *et al*., 2004). To further

characterize the epidermal changes we looked at PY-Stat3 staining in affected *Hnrnpd* ^{tm1Rjsc} mice. No staining was seen in unaffected skin (Figure S1c). In contrast, the thickened epidermis in acute lesions (Figure 2h) and skin neighboring lesions (Figure S1d) demonstrate strong PY-Stat3 staining. Increased neovascularization is seen by the large number of capillaries present close to dermoepidermal junction (Figure 2e) and as can be visualized by antibodies to CD31 (Figure 2i). Neutrophil aggregates composed of mounds of pykotic neutorphilic debris and eosinophilic serum can be seen above parakeratotic stratum corneum (Figure 2e and g). In addition to aggregates, neutrophil infiltration within the epidermis and dermis can be seen by antibodies to Gr-1 (Figure 2j). Staining for T cells demonstrates a large dermal infiltration and occasional epidermal infiltrate (Figure 2k). Antibodies to F4/80 demonstrate dermal macrophage infiltrate (Figure 2l). A moderate degree of eosinophil infiltration can be seen in chronic lesions (Figure 2m). Numerous dermal mast cells, some of which show degranulation, are evident in chronic lesions (Figure 2n) and the number mast cells correlate with chronicity of the lesion. Mast cell degranulation is caused by crosslinking of IgE receptors (Navi *et al*., 2007), thus we measured IgE serum levels in affected *Hnrnpd*^{tm1Rjsc} mice. Although no significant difference was seen between the serum IgE levels in wild-type (0.7 ± 0.3 μgml^{-1}) and unaffected *Hnrnpd* ^{tm1Rjsc} (1.2 ± 0.4 μgml^{-1}) mice 8–12 months of age, *Hnrnpd* ^{tm1Rjsc} mice of the same age with chronic dermatitis (CD) had significantly higher serum IgE levels (7.9 ± 5.5 μgml^{-1}) (Figure 2o). Furthermore, the inflammation in lesions in *Hnrnpd* ^{tm1Rjsc} mice was associated with a shift towards a Th_2 immune environment as was indicated by the decrease in IFN-γ (Th_1-specific cytokine) mRNA relative to IL4 (Th_2- specific cytokine) mRNA levels as compared to control biopsies from wild-type littermates (Figure 2p). The shift was observed in all periocular biopsies taken from affected *Hnrnpd* ^{tm1Rjsc} mice, with biopsies from earlier disease (mild blepharitis) displaying a greater Th_2 shift than biopsies taken from more progressed lesions (Figure 2p). In contrast, biopsies taken from unaffected ears of the same *Hnrnpd* ^{tm1Rjsc} mice showed no differences as compared to ears form wild-type littermate ears. In addition, biopsy of a *Hnrnpd* ^{tm1Rjsc} ear affected by dermatitis also exhibited a similar Th_2 shift. These results suggest that the onset and early progression of lesions is associated with a shift towards a Th_2 environment in *Hnrnpd* ^{tm1Rjsc} mice.

Increased contact hypersensitivity response in *Hnrnpd* ^{tm1Rjsc} mice

Given the eczematous and inflammatory nature of skin lesions *in Hnrnpd* ^{tm1Rjsc} mice, we next sought to investigate the CHS response, a good experimental model for T-cell-derived, cytokine-mediated skin inflammation (Watanabe *et al*., 2002). Sensitized *Hnrnpd* ^{tm1Rjsc} mice exhibit increased ear swelling and dense mononuclear cell infiltrate (Figure 3a–c) 24 hours after elicitation with DNFB as compared to wild-type littermate controls. No ear swelling was exhibited in nonsensitized *Hnrnpd*^{tm1Rjsc} mice and wild-type littermate controls treated with DNFB (Figure 3c), excluding the possibility that the increase in ear thickness was a result of irritation. The numbers of infiltrating macrophages and T cells, but not neutrophils were significantly increased in *Hnrnpd* ^{tm1Rjsc} ears 24 hours after elicitation as compared to that in wild-type controls (Figure 3d–f). To better characterize the nature of the response, inflammatory cytokine and chemokine levels in DNFB-elicited ears were assessed by quantitative (q) reverse transcriptase (RT)-PCR. The mRNA levels of TNF, IL1β, IL2, and monocyte chemoattractant protein 1 (MCP1; also known as CCL2) were

significantly increased, whereas IL1 receptor antagonist (IL1Ra) mRNA levels were substantially reduced in the ears of *Hnrnpd* ^{tm1Rjsc} mice (Figure 3g). The importance of TNF, IL1β, MCP1, and IL1Ra in regulating the CHS response and skin inflammation has been well established (Kondo *et al*., 1995; Mizumoto *et al*., 2001; Wang *et al*., 2003), validating and providing mechanistic insight into the enhanced CHS response seen in *Hnrnpd* ^{tm1Rjsc} mice. Furthermore, characterization of IFN-γ and IL4 mRNA levels in DNFB-elicited ears from *Hnrnpd* ^{tm1Rjsc} mice suggests a shift towards a Th_2 response as compared to that observed in wild-tye littermates. There was a fourfold decrease in the ratio of IFN-γ mRNA levels relative to IL4 mRNA levels in DNFB-elicited ears from *Hnrnpd* ^{tm1Rjsc} mice as compared to wild-type littermates (Figure 4h). In contrast, there was a threefold increase in the ratio of IFN-γ mRNA levels relative to IL4 mRNA levels in DNFB-elicited ears from *Hnrnpd* ^{tm1Rjsc} mice with CD.

To further delineate the role of HNRNPD in afferent and efferent phases of the CHS response, adoptive transfer experiments were performed. *Hnrnpd* ^{tm1Rjsc} and wild-type littermate donors were sensitized with DNFB. After 5 days, pooled purified T cells from draining lymph nodes of each group of sensitized mice were injected into the base of the ear of naïve wild-type mice. Cells from *Hnrnpd* ^{tm1Rjsc} mice were injected into the right ear and wild-type cells into the left ear of each recipient mouse. The recipient mouse was then immediately challenged with DNFB and ear thickness was measured 24 hours later. There was a slight but not significant increase in the ear thickness in ears receiving *Hnrnpd* ^{tm1Rjsc} T cells as compared to those receiving wild-type T cells (54.8±2.6 vs 51.8±2.2×10^{-2} mm; Figure 4a–c). We next assessed the effect of HNRNPD deficiency on the efferent or elicitation phase. Pooled purified T cells from draining lymph nodes of DNFB sensitized wild-type mice were injected into the base of right ears of naïve *Hnrnpd* ^{tm1Rjsc} and wild-type littermate recipient mice. As a control, the left ears were injected with purified T cells from lymph nodes of naïve wild-type mice. After transfer the ears of the mice were challenged with DNFB and ear thickness was measured. There was an increase in ear thickness in *Hnrnpd* ^{tm1Rjsc} recipients of sensitized wild-type T cells as compared to wild-type recipients (55.9±2.3 vs 49.6±2.2×10^{-2} mm, $P<0.05$; Figure 4d, e and h). DNFB-challenged left ears of recipient *Hnrnpd* ^{tm1Rjsc} and wild-type mice receiving T cells from naïve wild-type mice did not exhibit a CHS response (Figure 4f–h), excluding an irritation response as a source of ear swelling. These findings suggest that the increased CHS response in *Hnrnpd*^{tm1Rjsc} mice is primarily due to an enhanced efferent phase of the CHS response. This is concordance with the prolonged and increased production of TNF and IL1β, key effectors of the efferent phase of CHS (Nakae *et al*., 2003; Wang *et al*., 2003), in inflammatory cells from *Hnrnpd* ^{tm1Rjsc} mice (Lu *et al*., 2006).

p38 MAPK activation is required for increased CHS in *Hnrnpd* ^{tm1Rjsc} mice

The p38 mitogen-activated protein kinase (MAPK) has been demonstrated to be important in skin inflammatory diseases, CHS in mice (Takanami-Ohnishi *et al*., 2002), and serves as a therapeutic target for a variety of inflammatory diseases (Kumar *et al*., 2003). The p38 MAPK controls inflammation in part by regulating ARE-mediated mRNA decay (Takanami-Ohnishi *et al*., 2002). Therefore, we next evaluated the effect of pharmacological inhibition of the p38 MAPK with SB203580 (Kumar *et al*., 2003) on CHS elicitation in

sensitized-*Hnrnpd* ^{tm1Rjsc} mice. Pretreatment of sensitized mice with SB203580 before elicitation had a much greater antiinflammatory effect on the CHS response elicited in *Hnrnpd* ^{tm1Rjsc} mice as compared to wild-type littermates (Figure 5). The difference in ear thickness between ears pretreated with SB203580 and vehicle alone in *Hnrnpd* ^{tm1Rjsc} mice was twofold greater than the difference seen in wild-type mice (Figure 5a). Similarly the increase in mRNA levels of IL1β, IL6, and MCP1 exhibited post-CHS elicitation in *Hnrnpd* ^{tm1Rjsc} mice was reduced to levels comparable or below that seen in wild-type controls when *Hnrnpd* ^{tm1Rjsc} mice were pretreated with SB203580 before elicitation with DNFB (Figure 5b). Hence p38 MAPK inhibitors currently in clinical trails may hold even greater therapeutic potential in the treatment of inflammatory diseases, including inflammatory dermatoses, accompanied by loss-of-function *Hnrnpd* mutations.

Hnrnpd-deficient T cells are hyperproliferative

Given the importance of T cells in CHS and eczematous dermatitis in animal models (Leung *et al*., 2004), we assessed the effect of *Hnrnpd* deficiency on T-cell proliferation. T cells from unaffected animals were labeled with carboxyfluorescein diacetate succinimidyl ester (CSFE), then stimulated by TCR activation and analyzed by flow cytometry to assess cell division. T cells from *Hnrnpd* ^{tm1Rjsc} mice, particularly $CD4^+$ cells, divide more readily than wild-type T cells (Figure 6a). This difference is largest at lower levels of TCR activation. For example, at 72 hours after stimulation with 0.2 $\mu g ml^{-1}$ of antibody to CD3, 19% of $CD4^+$ cells from *Hnrnpd* ^{tm1Rjsc} mice entered their third division compared to only 10% of wild-type $CD4^+$ cells. In complementary experiments, isolated splenic $CD4^+$ T cells show increased [^{3}H]thymidine incorporation after stimulation (Figure 6b). In both assays, the greatest differences were observed in lower doses of an antibody to CD3, suggesting that $CD4^+$ T cells from *Hnrnpd* ^{tm1Rjsc} mice are more readily activated under suboptimal stimulation conditions. In accordance with these results, T cells from *Hnrnpd* ^{tm1Rjsc} mice produce significantly higher levels of IL2 than T cells from wild-type littermates in response to TCR activation (Figure 6c). This increase is detectable within 24 hours, at a time when it is evident by CSFE analysis that proliferation has not taken place. Silencing of HNRNPD expression in Jurkat T cells by shRNA results in a similar twofold increase in IL2 production as compared to Jurkat T cells treated with control knockdown vector (Figure 6d). Thus, the increase in IL2 production is dependent upon loss of *Hnrnpd* expression and is not a result of developmental differences of T cells in *Hnrnpd* ^{tm1Rjsc} mice.

Increased recruitment of *Hnrnpd* ^{tm1Rjsc} macrophages to sites of inflammation

Given the enhanced number of dermal macrophages in the CHS response and in skin lesions of *Hnrnpd* ^{tm1Rjsc} mice, we assessed the recruitment of macrophages to sites of inflammation in *Hnrnpd* ^{tm1Rjsc} mice by using a thioglycollate-induced peritonitis model. Although no difference was seen in the number of resident macrophage populations between *Hnrnpd* ^{tm1Rjsc} and wild-type mice, thioglycollate treatment resulted in a 60% increase in the number of $F4/80^+$ peritoneal macrophages in *Hnrnpd* mice (Figure 7a). This increase was even evident in 129S6-*Hnrnpd* ^{tm1Rjsc} mice (Figure 7b), a strain that has been reported to have a sharp defect in macrophage recruitment (White *et al*., 2002). Furthermore, 8 hours post-intraperitoneal (i.p.) lipopolysaccharide (LPS) challenge, *Hnrnpd* ^{tm1Rjsc} mice showed a 65% increase in the number of peripheral blood monocytes (Figure 7c), which coincides

with a twofold increase in serum MCP1 levels at 4 hours after challenge. These data, in addition to CHS response studies, suggest that in *Hnrnpd* ^{tm1Rjsc} mice there is an increase in the recruitment of macrophages to sites of inflammation, including the skin, in part due to increased MCP1 levels.

Subcutaneous injection of CCL27 and TNF in *Hnrnpd* ^{tm1Rjsc} mice results in inflammatory lesions similar to spontaneous eczematous dermatitis

To directly assay the role of T cell and macrophage recruitment in the formation of lesions seen in *Hnrnpd* ^{tm1Rjsc} mice, we injected mice with macrophage and skin T-lymphocyte homing chemokines, MCP1, and CCL27, respectively (Homey *et al*., 2002; Wang *et al*., 2006). Unaffected *Hnrnpd* ^{tm1Rjsc} and wild-type littermates were injected subcutaneously with MCP1 alone, MCP1 and TNF, CCL27 alone, CCL27 and TNF, TNF alone, or phosphate-buffered saline (PBS) as a control. Although no lesions were observed in wild-type mice, sites on *Hnrnpd* ^{tm1Rjsc} mice injected with MCP1 alone, MCP1 and TNF, or CCL27 and TNF, resulted in inflammatory lesions (Figure 8; Figure S2a).

It has been demonstrated in mice that T lymphocytes can be attracted to the skin by subcutaneous injection of CCL27 (Homey *et al*., 2002). Injection of CCL27 resulted in a large number of dermal T cells but did not result in epidermal changes (Figure S2b). However, sites injected with CCL27 and TNF resulted in inflammatory lesions in *Hnrnpd* ^{tm1Rjsc} mice. These lesions histologically resembled chronic spongiotic dermatitis, and were accompanied by a large infiltration of T lymphocytes and macrophages (Figure 8a–c). These lesions shared many similarities to chronic lesions seen in *Hnrnpd* ^{tm1Rjsc} mice, including marked acanthosis of the epidermis, hyperkeratosis, increased dermal capillary formation (Figure 8a and m), PY-Stat3 staining (Figure S2c), and large infiltrate of mast cells (Figure 8o). In contrast, infiltration of T cells and macrophages could be seen at sites of simultaneous injection of CCL27 and TNF in wild-type littermate controls although no epidermal changes were observed (Figure 8d–f).

Injection of MCP1 (Figure 8g–i) or MCP1 and TNF (Figure S2a, Figure 8n) also resulted in inflammatory lesion formation in *Hnrnpd* ^{tm1Rjsc} mice. Injection of MCP1 resulted in epidermal changes and massive infiltration of macrophages and T cells in *Hnrnpd* ^{tm1Rjsc} mice (Figure 8g–i). In contrast, injection of MCP1 in wild-type mice resulted in a robust macrophage infiltrate but virtually no T cells (Figure 8j–l). We speculate that recruited macrophages in *Hnrnpd* ^{tm1Rjsc} mice are unable to properly regulate their proinflammatory response, leading to a cyclical amplification of inflammatory processes including T-cell recruitment and epidermal changes. Histological examination of lesions at sites of MCP1 injection however showed a number of differences from lesions seen in *Hnrnpd* ^{tm1Rjsc} mice. Lesions caused by MCP1 injection histologically resemble interface dermatitis with a large inflammatory cell infiltrate (Figure 8g and n) and in extreme cases, exhibit vacuolar formation at the dermoepidermal junction (Figure 8n). Furthermore, these lesions show a smaller degree of epidermal acanthosis and hyperkeratosis, no PY-Stat3 staining (Figure S2c), and a smaller number of mast cells as compared to lesions formed by injection of CCL27 and TNF (Figure 8o). These studies suggest that the order of leukocyte recruitment may be important in lesion formation. Furthermore, they suggest that T-cell recruitment

concomitant with an inflammatory trigger, such as TNF secretion, are important in causing the lesions seen in *Hnrnpd* ^{tm1Rjsc} mice.

DISCUSSION

Hnrnpd ^{tm1Rjsc} mice develop eczematous lesions which share several features resembling human AD. The skin disease seen in *Hnrnpd* ^{tm1Rjsc} mice fulfills three major diagnostic criteria, including pruritus, CD, and family history of cutaneous atopy (dermatitis), as well as four minor criteria, including elevated serum IgE levels, staphylococcal skin infection, conjunctivitis, and xerosis (Hanifin and Rajka, 1980). We acknowledge that further characterization of *Hnrnpd* ^{tm1Rjsc} mice is needed before it can serve as model for human AD. However many relevant features including, elevated number of dermal T cells, mast cells, macrophages, and serum IgE levels, as well as, eczematous epidermal changes, shift towards a Th_2 microenvironment in acute lesions, pruritus, and sensitivity to dexamethasone suggest the *Hnrnpd* ^{tm1Rjsc} mouse model may be useful in the study of AD.

Several mouse models reproducing features of human AD have been described, including NC/Nga mice (Matsuda *et al*., 1997), transgenic mouse models with expression of human APOC1 (*Tg(APOC1)1Lmh*) (Nagelkerken *et al*., 2008), and targeted expression of IL4 (*Tg(KRT14-Il4)1LuXu*) (Chan *et al*., 2001) or IL18 (*Tg(KRT14-Il18)1Miz*) (Konishi *et al*., 2002) to the basal layer using a keratin 14 promoter. *Hnrnpd* ^{tm1Rjsc} mice share several features with these models, including pruritis, CD characterized by acanthotic epidermis, elevated serum IgE levels, as well as dermal infiltrate of T cell, mast cell, macrophage, and eosinophils. *Hnrnpd*^{tm1Rjsc} mouse model, similar to other spontaneous models (Shiohara *et al*., 2004), is hampered by lack of complete penetrance and variability in the age of onset of dermatitis phenotype. However, these limitations can be eased by using hapten-induced models (Shiohara *et al*., 2004), as well as induced models of dermatitis described in this report that will provide a controlled setting to investigate the pathophysiology of inflammatory lesions.

AD and allergic contact dermatitis are both eczematous diseases mediated through immune mechanisms (Akhavan and Cohen, 2003). *Hnrnpd* ^{tm1Rjs} mice exhibit a enhance CHS response suggesting a greater susceptibility to hapten-specific T-cell-mediated skin inflammation, such as allergic contact dermatitis (Saint-Mezard *et al*., 2004). This report focuses on similarities between the pruritic inflammatory skin disease in *Hnrnpd* ^{tm1Rjs} mice and human AD mainly due to the increased serum IgE levels and dermal mast cells in affected mice. However, we acknowledge that the overlap in the histopathology of human atopic and allergic contact dermatitis as well as work from mice showing an important role for IgE (Bryce *et al*., 2004) and mast cells (Yokozeki *et al*., 2003) in CHS does not allow this distinction to be clearly made at this time.

The lesions occurring in our *Hnrnpd* ^{tm1Rjsc} mice were predominately seen in the facial region very similar to NC/Nga (Matsuda *et al*., 1997) and *Tg(KRT14-Il4)1LuXu* (Chan *et al*., 2001) mice. We speculate that the dominance of lesions in the facial region of *Hnrnpd*^{tm1Rjs} mice may be a result of mechanical stress created by grooming, although we can not rule out other possible environmental triggers, including a pathological response to normal flora with

age. Once lesions are initiated the increased scratching presumably aids in the progression of lesions. The background strain of our *Hnrnpd* ^{tm1Rjs} mice may also contribute to the predilection of periocular involvement. The 129P3/J, a parental strain of our 129S6- or B6;129S6-*Hnrnpd* ^{tm1Rjs} mice, and BALB/cBy, the background of *Tg(KRT14-Il4)1LuXu* (Chan *et al*., 2001) mice, have been reported to have increased incidence for ulcerative blepharitis (Sundberg *et al*., 1991). Furthermore, the 129 strain has been reported to exhibit more severe ocular changes and blepharitis in an experimental model of systemic lupus erythematosus (Chan *et al*., 1995). Although the 129 background may impact susceptibility of periocular involvement, lesion are not limited to presumably being initiated with periocular involvement, as 25% of affected mice present with dermatitis without periocular involvement.

We have previously shown that *Hnrnpd*-deficient macrophages are unable to rapidly degrade TNF and IL1β mRNAs following induction, leading to their overexpression (Lu *et al*., 2006). Furthermore, we have also previously shown that *Hnrnpd* preferentially binds to and controls the turnover of a number of ARE-containing transcripts that contain overlapping AUUUA pentamers (Lu *et al*., 2006). TNF, IL1β, and IL2 mRNAs all contain overlapping AUUUA pentamers (Halees *et al*., 2008) and are increased 24 hours post-CHS elicitation in *Hnrnpd* ^{tm1Rjs} mice as compared to wild-type littermates. The CHS studies in this report were performed with DNFB, a hapten that has been previously shown to predominantly elicit a Th_1 response (Dearman *et al*., 1997; Wang *et al*., 2000). Measurement of the ratio of IL4 mRNA relative to IFN-γ mRNA levels in DNFB-elicited ears suggest that the inflammatory response in *Hnrnpd* ^{tm1Rjs} mice is shifted towards a Th_2 response. Future studies with a hapten that predominantly elicit a Th_2 response will better allow the characterization of a Th_2-mediated response as well as Th_2-specific cytokine mRNAs that may be regulated by HNRNPD. The IL4 mRNA, a pivotal enhancer of the Th_2 response, contains overlapping AUUUA pentamers (Halees *et al*., 2008), is bound by HNRNPD (Yarovinsky *et al*., 2006), and is suggested to be a target of *Hnrnpd* regulation (Sadri *et al*., 2008). In agreement with a proposed role of HNRNPD in IL4 regulation, mice transgenic for murine IL4 (FVB/N-*Tg(Igh-Il4)1Led*) developed blepharitis and periocular skin inflammation when maintained in a pathogen-free facility (Tepper *et al*., 1990) similar to *Hnrnpd* ^{tm1Rjs} mice. Hence, future studies are needed to validate the role of HNRNPD in the control of other cytokines encoded by ARE-containing mRNAs with overlapping AUUUA pentamers, such as IL4 and IL12. In contrast to the CHS response associated with a shift towards a Th_2 response in *Hnrnpd* ^{tm1Rjsc} mice before onset of overt dermatitis, *Hnrnpd* ^{tm1Rjsc} mice with CD elicit a CHS response that is more strongly shifted towards a Th_1 response. In addition, measurement of IL4 and IFN-γ mRNA levels from acute lesions in *Hnrnpd* ^{tm1Rjsc} mice suggest that lesion formation and early progression is associated with a shift towards a Th_2 microenvironment. Taken together, these results suggest a possible biphasic response in *Hnrnpd* ^{tm1Rjsc} mice similar to that seen in AD (Leung *et al*., 2004), in which a Th_2 response predominates in acute lesions followed by a switch to a Th_1 response that predominates in chronic lesions. Further in depth characterization of acute and chronic stage lesions will be important in more closely evaluating the immunological environment (Th_1 or Th_2) of these lesions at various stages of disease progression.

It is interesting to note that whereas TNF, IL1*β*, and IL2 mRNAs all contain the canonical AUUUA motif, the mRNAs encoding MCP1 and IL1Ra do not. The canonical AUUUA motif is not the only motif recognized by HNRNPD, however, and we have confirmed reports that HNRNPD controls the stability of p21, a mRNA that does not contain this classical motif (Lal *et al*., 2004). Furthermore, a screen for AUF1 ligands in mitogen-activated peripheral blood mononuclear cells revealed MCP1, IL1Ra, and p21 as targets of HNRNPD (Bhattacharya *et al*., 1999). It is believed that ARE flanking sequences and higher order structural determinants formed by mRNAs are also important in determining the binding of ARE-binding proteins to AREs, and may explain the diversity of AUF1 targets (Barreau *et al*., 2005). Conversely, the differences in expression in CHS studies could result from secondary affects due to altered expression of direct HNRNPD targets, such as TNF and IL1*β*, which have been shown to have a direct impact on the expression of IL6, MCP1, and IL1Ra (Gu *et al*., 1999; Palmer *et al*., 2007). The generation of *Tnfrsf1a*Il1r1*Hnrnpd* triple knockout mice will help to address this question.

CCL27 is produced by keratinocytes and serves as a skin-specific chemokine for T cells that express CCR10 (Homey *et al*., 2002). Subcutaneous injection of recombinant CCL27 has been shown to induce the recruitment of T cells to the site of injection (Homey *et al*., 2002). Although the direct role of CCL27 in human AD has not been established, recent studies suggest CCL27 may be involved in skin inflammation in human AD. Lesions of human AD show increased expression of CCL27 expression (Homey *et al*., 2002). Furthermore, serum levels of CCL27 are elevated in patients with AD (Kakinuma *et al*., 2003; Hon *et al*., 2004) and the elevation is correlated with disease severity (Hon *et al*., 2004). In addition, subcutaneous injection of neutralizing antibodies to CCL27 in early AD-like lesions in the *Tg(KRT14-Il4)1LuXu* mouse model resulted in reduced clinical progression of inflammation accompanied with reduced number of T and mast cells, as well as, decreased epidermal acanthosis (Chen *et al*., 2006). Although a large infiltration of T cells could be seen with intradermal injection of CCL27 in *Hnrnpd* ^{tm1Rjs} mice, few dermal macrophages and mast cells were seen and epidermal changes were not observed. However, intradermal injection of CCL27 and TNF in *Hnrnpd* ^{tm1Rjs} mice results in eczetamous dermatitis with a large dermal infiltrate of T cells, macrophages, and mast cells closely resembling spontaneous dermatitis seen in *Hnrnpd* ^{tm1Rjs} mice. These data suggest that both CCL27-responsive T cells and a proper proinflammatory environment, as created by TNF, are important in leading to subsequent leukocyte infiltration and epidermal morphological changes in *Hnrnpd* ^{tm1Rjs} mice. Proinflammatory cytokines, such as TNF, are important in endothelial activation resulting in the expression of adhesion molecules that enable leukocyte infiltration (de Vries *et al*., 1998), as well as activating keratinocytes to produce chemokines and undergo morphological changes (Banno *et al*., 2004). Differences seen in functional properties of *Hnrnpd*-deficient T cells and macrophages suggest altered inflammatory and immunological pathways in *Hnrnpd* ^{tm1Rjsc} mice that may predispose these mice to inflammatory skin lesions. Furthermore, induced lesions by CCL27 and TNF injection share similarities with our current understanding of the early events of human AD. These early events have been characterized by an upregulation of proinflammatory cytokines, TNF and IL1*β*, that together with chemokines lead to the recruitment of different subset of leukocytes, including CCL27-responsive T cells (Avgerinou *et al*., 2008). Hence, our experimentally induced model in

Hnrnpd ^{tm1Rjsc} mice provides a controlled assay to further study the initiation events, progression, and pathophysiology of these inflammatory lesions.

In summary, the *Hnrnpd* ^{tm1Rjsc} mouse model exhibiting pruritic inflammatory skin disease, enhanced CHS, and experimentally induced dermatitis will help in investigating the targets of *Hnrnpd* and the consequence of aberrant mRNA turnover of these targets in regulating skin inflammation. This understanding may provide insight into the pathophysiology and therapeutic strategy of similar human dermatoses, such AD.

MATERIALS AND METHODS

Mice

The B6;129S6- and 129S6-*Hnrnpd*^{tm1Rjsc} and corresponding wild-type mice were derived and genotyped as previously described (Lu *et al*., 2006). Chimeric founder males were breed with C57BL/6 (B6) wild-type females to generate heterozygotes on a mixed B6;129S6. These heterozygotes were crossed to produce *Hnrnpd*^{tm1Rjsc} homozygotes and wild-type littermates on a mixed B6;129S6 background. All mice are kept under specific pathogen-free conditions. All animal protocols were approved by the NYU Institutional Animal Care and Use Committee.

Immunohistochemistry, immunofluorescence staining, and flow cytometry

Paraffin-embedded skin specimens were stained with antibodies to PY-Stat3 (Cell Signaling Technology, Danvers, MA) as described (Sadri *et al*., 2008). Frozen sections were stained with antibodies specific to F4/80 (BM8), CD3ε (17A2), CD31 (390), and Gr-1 (RB6-8C5) (eBioscience, San Diego, CA). In some sections, nuclei were counterstained with ToPro3 (Molecular Probes, Carlsbad, CA). For eosinophil identification frozen sections were pretreated with 10mM potassium cyanide solution to block myeloperoxidase activity and then eosinophil peroxidase was probed for with DAB-Ni. Cells from spleens, lymph nodes, and peritoneal lavage were stained as described (Lu *et al*., 2006) with antibodies from Pharmingen (BD Biosciences, San Jose, CA) to CD4 (GK1.5) and CD8 (53–6.72), antibodies from eBioscience to CD3ε (145-2C11), TCRβ (H57-597), and F4/80 (BM8). Samples were analyzed using a FACSCalibur flow cytometer (BD Biosciences) and FlowJo software (TreeStar, Ashland, OR).

ELISA

For serum IgE levels, microtiter plates were coated with anti-mouse IgE (R35-72; Pharmingen), followed by sequential incubation of serially diluted purified mouse IgE (C38-2; Pharmingen) or sera from mice (tested at 1:100, 1:1,000, and 1:10,000 dilutions), biotinylated anti-mouse IgE (23G3; eBioscience), streptavidin-HRP (eBioscience), and then TMB substrate solution (eBioscience). Total serum levels were calculated using standard curve generated from optical density readings at 450nm for purified mouse IgE.

Mouse CHS model

After being anesthetized with ketamine, healthy B6;129S6- *Hnrnpd*^{tm1Rjsc} and littermate sex-matched wild-type mice 6 months of age were sensitized on shaved abdomen skin with

30 μl of 0.5%. DNFB (Sigma) in 4:1 acetone and olive oil solution (A/O). At 5 days after sensitization, the mice were challenged on each side of the right ear with 10 μl of 0.2% DNFB in A/O solution. As the control, 10 μl of A/O solution was added to each side of the left ear. At 24 hours after challenge the thickness of the ear was measured using an engineer's micrometer (Ozaki Manufacturing, Tokyo, Japan). For the determination of the effect of SB203580 (#599389, Calbiochem, Gibbstown, NJ), 10 μl of 10μM SB203580 diluted in A/O solution was applied to each side of the right ear of sensitized mice 30 minutes before challenge. As a control, left ears were pretreated before challenge with A/O solution. Samples from ears 24 hours after challenge were used for qRT-PCR cytokine detection and immunohistochemistry.

For assaying the role of *Hnrnpd* on the afferent phase of CHS, B6;129S6-*Hnrnpd* ^{tm1Rjsc} and littermate sex-matched wild-type mice 6 months of age were sensitized with 0.5% DNFB on shaved abdomen and ears. Pooled purified T cells (by negative selection with $B220^+$ and $Mac1^+$ microbeads and MACS system; Miltenyi Biotec, Auburn, CA) from draining lymph nodes of each group were injected into the base of the ear (10^5 T cells in 10 μl of PBS) of naïve B6;129S6 wild-type mice 8 months of age. CHS was elicited and measured as described above.

For assaying the role of *Hnrnpd* on the efferent phase of CHS, wild-type B6;129S6 mice 6 months of age were sensitized with 0.5% DNFB. Pooled purified T cells (by negative selection as stated above with MACS system) from draining lymph nodes were injected into the base of the right ear (10^5 T cells in 10 μl of PBS) of naïve B6;129S6-*Hnrnpd* ^{tm1Rjsc} and littermate sex-matched wild-type mice 6 months of age. Pooled T cells from unsensitized donor mice were injected into the left ears of naïve recipients as controls. CHS was elicited and measured as described above.

RT–PCR detection of cytokine and chemokine mRNAs

Samples were taken from control and challenged ears 24 hours after challenge, homogenized in Trizol (Invitrogen, Carlsbad, CA) and mRNA was extracted according to manufacturer's instructions. Cytokine and chemokine levels were determined by qRT-PCR using the Roche LightCycler system with a SYBR-Green Master kit (Roche Molecular Biochemicals, Mannheim, Germany), and gene-specific primers are available upon request. C_T values were used to calculate relative values and were normalized to C_T values for cyclophilin A and HPRT. The normalized value for a given transcript from the ear of an *Hnrnpd* ^{tm1Rjsc} mouse was compared to that of its wild-type littermate. For calculations of the ratio of IFN-γ to IL4 mRNA levels, mRNA was extracted from 4mm punch biopsies or ears as described above. The C_T value for IFN-γ was normalized to the C_T value for IL4 for each sample and the $\Delta\Delta C_T$ method was used to calculate ratios.

Proliferation assays and IL2 ELISA

To trace cell division, lymph node and spleen cells were purified from 4-month-old B6;129S6 mice and labeled with 10 μM CSFE (Molecular Probes) at room temperature for 10 minutes. Cells were washed in complete RPMI 1,640 media (Lu *et al*., 2006) and stimulated in 12-well plates (5×10^5 cells per well) coated with anti-CD3ε (145-2C11;

eBioscience) at concentrations of 0.04, 0.2, 1, and 5 μgml^{-1} for 24 or 72 hours. Progression of cell division was determined by flow cytometry after cell-surface staining with antibodies to CD4 and CD8. In [^{3}H]thymidine proliferation assays, splenocyte T cells were purified by using antibody-bead depletion using B220 microbeads, followed by positive selection with CD4 microbeads (MACS). Purified CD4$^+$ T cells resuspended in complete RPMI 1,640 media were plated in triplicate in 96-well plate coated with various concentrations of anti-CD3ε (145-2C11; eBioscience) and anti-CD28 (37.15; eBioscience) for 48 hours. During the last 8 hours the cultures were pulsed with 1 μCi per well [^{3}H]thymidine, and cells were then harvested onto glass-fiber filters, and thymidine incorporation was measured using a scintillation counter. To measure IL2 production, lymph node and spleen cells were purified and stimulated in 48-well plates (1×10^5 cells per well) coated with anti-CD3ε (145-2C11; eBioscience) at concentrations of 0, 0.04, 0.2, 1, and 5 μgml^{-1} for 24 hours. Supernatants were collected and mouse IL2 ELISA (eBioscience) was performed according to manufacturer's instructions.

Hnrnpd expression was knocked down in Jurkat T cells using a control and *Hnrnpd*-directed shRNA^{mir} retroviral vectors (Open Biosystems, Huntsville, AL) according to manufacturer's instructions. Immunoblot analysis was performed following standard protocols with antibodies to *Hnrnpd* (995), HuR (3A2), and TIAR (C-18) from Santa Cruz Biotechnology (Santa Cruz, CA). For IL2 production studies, Jurkat T cells were stimulated in 96-well plates (1×10^5 cells per well) coated with anti-CD3 (OKT-3; eBioscience) and treated with phorbol myristate acetate (PMA) (10 ng ml^{-1}). Supernatants were collected and human IL2 ELISA (eBioscience) was performed according to manufacturer's instructions.

Macrophage recruitment

Mice were administered 1ml of 4% thioglycollate broth i.p., and 72 hours later were killed. Cells were recovered by peritoneal lavage, counted using a hemocytometer, stained with an antibody to F4/80 (BM8), and analyzed by flow cytometry as described (Lu *et al*., 2006). The number of macrophages was calculated based on proportion of F4/80$^+$ cells. For systemic macrophage recruitment assay, mice were injected i.p. with LPS (20 μg g^{-1}), tail bleed at 4 hours, and 8 hours later were killed. Monocyte counts were performed on blood samples collected 8 hours post-LPS challenge (Ani Lytics Inc., Gaithersburg, MD). MCP1 levels were measured on serum from samples 4 hours after challenge using Mouse Cytokine Array blots (RayBiotech Inc., Norcross GA) according to the manufacturer's instructions.

Intradermal injections with MCP1, TNFα, and CCL27

B6;129S6-*Hnrnpd* ^{tm1Rjsc} and wild-type littermate mice 8–12 months of age that showed no dermatitis were subcutaneously injected with either CCL27 (2.5 μg; PeproTech, Rocky Hill, NJ), CCL27 (2.5 μg) + rat rTNF (5,000 U; Pepro-Tech), rJE/MCP1 (0.2 μg; Pepro-Tech), rJE/MCP1 (0.2 μg) + rTNF (5,000 U), rTNF (5,000 U), or PBS control diluted in 100 μl of PBS at six specific and separate spots on their dorsum. At 10 days after treatment, mice were killed, and injected sites were excised and examined by immunohistochemistry and immunoflourescence.

Administration of dexamethasone

Dexamethasone (2 $\mu g g^{-1}$; Phoenix Scientific, St. Joseph, MO) was administered s.q. everyday to back scruff for a period of 5 days and treated in tapering dose regimen (sequential twofold decrease for 4 days) until they were no longer treated. Other mice were treated daily with topical application of *Panalog* Cream (Triamcinolone; Fort Dodge Animal Health, Fort Dodge, IA) for 7 days. The progression and severity of lesions was observed daily during and for 2 weeks post-treatment for both topical and subcutaneous treatment groups.

Statistical analysis

Data are presented as mean±SD for statistical comparison of two samples, the two-tailed Student's *t*-test was used for evaluation. Incidence of dermatitis was presented by Kaplan–Meier and significance was evaluated using Log-rank test.

Supplementary Material

Refer to Web version on PubMed Central for supplementary material.

Acknowledgments

We thank Dr Cindy A Loomis, Dr Marjana Tomic, and Dr Scott Sanders for their thoughtful insight and review of the pathology. We thank Timothy Macatee and the Histology Core Facilities at NYU for assistance in preparing slides. We thank Dr Doris Tse and her staff at the Center for AIDS Research at NYU for assistance with FACS analysis. Purchase of the confocal microscope was funded by a Shared Instrumentation Grant from the NIH (S10 RR017970). This work was supported by a grant from the NIH (RJS) and an NIH T32 training grant (NS).

Abbreviations

AD	atopic dermatitis
ARE	AU-rich element
Auf1	ARE/poly-(U) binding degradation factor 1
CHS	contact hypersensitivity
CSFE	carboxyfluorescein diacetate succinimidyl ester
H/E	hematoxylin/eosin
Hnrnpd	heterogeneous nuclear riboncleoprotein D
IL1Ra	IL1 receptor antagonist
LPS	lipopolysaccharide
MAPK	mitogen-activated protein kinase
MCP1	monocyte chemoattractant protein 1
PBS	phosphate-buffered saline
qRT-PCR	quantitative reverse transcriptase-PCR
Stat3	signal transducer and activator of transcription 3

TNFα tumor-necrosis factor-α

References

Akhavan A, Cohen SR. The relationship between atopic dermatitis and contact dermatitis. Clin Dermatol. 2003; 21:158–62. [PubMed: 12706333]

Avgerinou G, Goules AV, Stavropoulos PG, Katsambas AD. Atopic dermatitis: new immunologic aspects. Int J Dermatol. 2008; 47:219–24. [PubMed: 18289319]

Banno T, Gazel A, Blumenberg M. Effects of tumor necrosis factor-alpha (TNF alpha) in epidermal keratinocytes revealed using global transcriptional profiling. J Biol Chem. 2004; 279:32633–42. [PubMed: 15145954]

Barreau C, Paillard L, Osborne HB. AU-rich elements and associated factors: are there unifying principles? Nucleic Acids Res. 2005; 33:7138–50. [PubMed: 16391004]

Bhattacharya S, Giordano T, Brewer G, Malter JS. Identification of AUF-1 ligands reveals vast diversity of early response gene mRNAs. Nucleic Acids Res. 1999; 27:1464–72. [PubMed: 10037807]

Boguniewicz M, Schmid-Grendelmeier P, Leung DY. Atopic dermatitis. J Allergy Clin Immunol. 2006; 118:40–3. [PubMed: 16815136]

Bryce PJ, Miller ML, Miyajima I, Tsai M, Galli SJ, Oettgen HC. Immune sensitization in the skin is enhanced by antigen-independent effects of IgE. Immunity. 2004; 20:381–92. [PubMed: 15084268]

Chan CC, Gery I, Kohn LD, Nussenblatt RB, Mozes E, Singer DS. Periocular inflammation in mice with experimental systemic lupus erythematosus. A new experimental blepharitis and its modulation. J Immunol. 1995; 154:4830–5. [PubMed: 7722331]

Chan KS, Sano S, Kiguchi K, Anders J, Komazawa N, Takeda J, et al. Disruption of Stat3 reveals a critical role in both the initiation and the promotion stages of epithelial carcinogenesis. J Clin Invest. 2004; 114:720–8. [PubMed: 15343391]

Chan LS, Robinson N, Xu L. Expression of interleukin-4 in the epidermis of transgenic mice results in a pruritic inflammatory skin disease: an experimental animal model to study atopic dermatitis. J Invest Dermatol. 2001; 117:977–83. [PubMed: 11676841]

Chen L, Lin SX, Agha-Majzoub R, Overbergh L, Mathieu C, Chan LS. CCL27 is a critical factor for the development of atopic dermatitis in the keratin-14 IL-4 transgenic mouse model. Int Immunol. 2006; 18:1233–42. [PubMed: 16735375]

de Vries IJ, Langeveld-Wildschut EG, van Reijsen FC, Dubois GR, van den Hoek JA, Bihari IC, et al. Adhesion molecule expression on skin endothelia in atopic dermatitis: effects of TNF-alpha and IL-4. J Allergy Clin Immunol. 1998; 102:461–8. [PubMed: 9768589]

Dearman RJ, Smith S, Basketter DA, Kimber I. Classification of chemical allergens according to cytokine secretion profiles of murine lymph node cells. J Appl Toxicol. 1997; 17:53–62. [PubMed: 9048228]

Gu L, Tseng SC, Rollins BJ. Monocyte chemoattractant protein-1. Chem Immunol. 1999; 72:7–29. [PubMed: 10550927]

Halees AS, El-Badrawi R, Khabar KS. ARED organism: expansion of ARED reveals AU-rich element cluster variations between human and mouse. Nucleic Acids Res. 2008; 36:D137–40. [PubMed: 17984078]

Hanifin JM, Rajka G. Diagnostic features of atopic dermatitis. Acta Derm Venereol (Stockh). 1980; 92(Suppl):44–7.

Hoffjan S, Epplen JT. The genetics of atopic dermatitis: recent findings and future options. J Mol Med. 2005; 83:682–92. [PubMed: 15902388]

Homey B, Alenius H, Muller A, Soto H, Bowman EP, Yuan W, et al. CCL27-CCR10 interactions regulate T cell-mediated skin inflammation. Nat Med. 2002; 8:157–65. [PubMed: 11821900]

Hon KL, Leung TF, Ma KC, Li AM, Wong Y, Fok TF. Serum levels of cutaneous T-cell attracting chemokine (CTACK) as a laboratory marker of the severity of atopic dermatitis in children. Clin Exp Dermatol. 2004; 29:293–6. [PubMed: 15115514]

Kakinuma T, Saeki H, Tsunemi Y, Fujita H, Asano N, Mitsui H, et al. Increased serum cutaneous T cell-attracting chemokine (CCL27) levels in patients with atopic dermatitis and psoriasis vulgaris. J Allergy Clin Immunol. 2003; 111:592–7. [PubMed: 12642842]

Kondo S, Pastore S, Fujisawa H, Shivji GM, McKenzie RC, Dinarello CA, et al. Interleukin-1 receptor antagonist suppresses contact hypersensitivity. J Invest Dermatol. 1995; 105:334–8. [PubMed: 7665908]

Konishi H, Tsutsui H, Murakami T, Yumikura-Futatsugi S, Yamanaka K, Tanaka M, et al. IL-18 contributes to the spontaneous development of atopic dermatitis-like inflammatory skin lesion independently of IgE/stat6 under specific pathogen-free conditions. Proc Natl Acad Sci USA. 2002; 99:11340–5. [PubMed: 12151598]

Kumar S, Boehm J, Lee JC. p38 MAP kinases: key signalling molecules as therapeutic targets for inflammatory diseases. Nat Rev Drug Discov. 2003; 2:717–26. [PubMed: 12951578]

Lal A, Mazan-Mamczarz K, Kawai T, Yang X, Martindale JL, Gorospe M. Concurrent versus individual binding of HuR and AUF1 to common labile target mRNAs. EMBO J. 2004; 23:3092–102. [PubMed: 15257295]

Leung DY, Boguniewicz M, Howell MD, Nomura I, Hamid QA. New insights into atopic dermatitis. J Clin Invest. 2004; 113:651–7. [PubMed: 14991059]

Lu JY, Sadri N, Schneider RJ. Endotoxic shock in AUF1 knockout mice mediated by failure to degrade proinflammatory cytokine mRNAs. Genes Dev. 2006; 20:3174–84. [PubMed: 17085481]

Lu JY, Schneider RJ. Tissue distribution of AU-rich mRNA-binding proteins involved in regulation of mRNA decay. J Biol Chem. 2004; 279:12974–9. [PubMed: 14711832]

Matsuda H, Watanabe N, Geba GP, Sperl J, Tsudzuki M, Hiroi J, et al. Development of atopic dermatitis-like skin lesion with IgE hyperproduction in NC/Nga mice. Int Immunol. 1997; 9:461–6. [PubMed: 9088984]

Mizumoto N, Iwabichi K, Nakamura H, Ato M, Shibaki A, Kawashima T, et al. Enhanced contact hypersensitivity in human monocyte chemoattractant protein-1 transgenic mouse. Immunobiology. 2001; 204:477–93. [PubMed: 11776402]

Nagelkerken L, Verzaal P, Lagerweij T, Persoon-Deen C, Berbee JF, Prens EP, et al. Development of atopic dermatitis in mice transgenic for human apolipoprotein C1. J Invest Dermatol. 2008; 128:1165–72. [PubMed: 18049452]

Nakae S, Komiyama Y, Narumi S, Sudo K, Horai R, Tagawa Y, et al. IL- 1-induced tumor necrosis factor-alpha elicits inflammatory cell infiltration in the skin by inducing IFN-gamma-inducible protein 10 in the elicitation phase of the contact hypersensitivity response. Int Immunol. 2003; 15:251–60. [PubMed: 12578855]

Navi D, Saegusa J, Liu FT. Mast cells and immunological skin diseases. Clin Rev Allergy Immunol. 2007; 33:144–55. [PubMed: 18094953]

Palmer G, Talabot-Ayer D, Kaya G, Gabay C. Type I IL-1 receptor mediates IL-1 and intracellular IL-1 receptor antagonist effects in skin inflammation. J Invest Dermatol. 2007; 127:1938–46. [PubMed: 17476299]

Saint-Mezard P, Rosieres A, Krasteva M, Berard F, Dubois B, Kaiserlian D, et al. Allergic contact dermatitis. Eur J Dermatol. 2004; 14:284–95. [PubMed: 15358566]

Sano S, Chan KS, Carbajal S, Clifford J, Peavey M, Kiguchi K, et al. Stat3 links activated keratinocytes and immunocytes required for development of psoriasis in a novel transgenic mouse model. Nat Med. 2005; 11:43–9. [PubMed: 15592573]

Shiohara T, Hayakawa J, Mizukawa Y. Animal models for atopic dermatitis: are they relevant to human disease? J Dermatol Sci. 2004; 36:1–9. [PubMed: 15488700]

Sundberg JP, Brown KS, Bates R, Cunliffe-Beamer TL, Bedigian H. Suppurative conjunctivitis and ulcerative blepharitis in 129/J mice. Lab Anim Sci. 1991; 41:516–8. [PubMed: 1666162]

Takanami-Ohnishi Y, Amano S, Kimura S, Asada S, Utani A, Maruyama M, et al. Essential role of p38 mitogen-activated protein kinase in contact hypersensitivity. J Biol Chem. 2002; 277:37896–903. [PubMed: 12138127]

Tepper RI, Levinson DA, Stanger BZ, Campos-Torres J, Abbas AK, Leder P. IL-4 induces allergic-like inflammatory disease and alters T cell development in transgenic mice. Cell. 1990; 62:457–67. [PubMed: 2116236]

Wang B, Esche C, Mamelak A, Freed I, Watanabe H, Sauder DN. Cytokine knockouts in contact hypersensitivity research. Cytokine Growth Factor Rev. 2003; 14:381–9. [PubMed: 12948522]

Wang B, Fujisawa H, Zhuang L, Freed I, Howell BG, Shahid S, et al. CD4+ Th1 and CD8+ type 1 cytotoxic T cells both play a crucial role in the full development of contact hypersensitivity. J Immunol. 2000; 165:6783–90. [PubMed: 11120799]

Wang H, Peters T, Kess D, Sindrilaru A, Oreshkova T, Van Rooijen N, et al. Activated macrophages are essential in a murine model for T cell-mediated chronic psoriasiform skin inflammation. J Clin Invest. 2006; 116:2105–14. [PubMed: 16886059]

Watanabe H, Unger M, Tuvel B, Wang B, Sauder DN. Contact hypersensitivity: the mechanism of immune responses and T cell balance. J Interferon Cytokine Res. 2002; 22:407–12. [PubMed: 12034022]

White P, Liebhaber SA, Cooke NE. 129X1/SvJ mouse strain has a novel defect in inflammatory cell recruitment. J Immunol. 2002; 168:869–74. [PubMed: 11777984]

Yarovinsky TO, Butler NS, Monick MM, Hunninghake GW. Early exposure to IL-4 stabilizes IL-4 mRNA in CD4+ T cells via RNA-binding protein HuR. J Immunol. 2006; 177:4426–35. [PubMed: 16982877]

Yokozeki H, Wu MH, Sumi K, Igawa K, Miyazaki Y, Katayama I, et al. Th2 cytokines, IgE and mast cells play a crucial role in the induction of para-phenylenediamine-induced contact hypersensitivity in mice. Clin Exp Immunol. 2003; 132:385–92. [PubMed: 12780683]

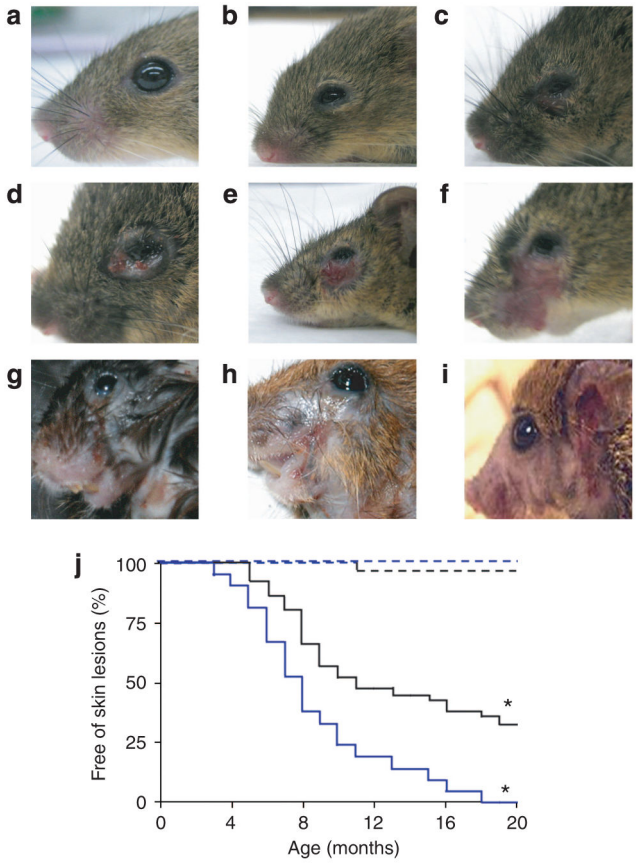

Figure 1. Appearance and incidence of dermatitis in *Hnrnpd*^{tm1Rjsc} mice

(**a**) Wild-type mouse (12-month old). (**b**–**f**) Representative pictures of increasing progression of disease severity in *Hnrnpd*^{tm1Rjsc} mice; (**b**, **c**) 3-month old with blepharitis and periocular edema; (**d**) 5-month old with severe blepharitis, serous exudates, and crust formation; (**e**, **f**) 6-month old with lesions spread to contiguous tissue and associated with excoriations and crusting. (**g**–**i**) Chronic lesions in 12-month-old *Hnrnpd*^{tm1Rjsc} mice associated with lichenification, erosion, crusting, and excoriations. (**j**) Incidence of dermatitis in B6;129S6-*Hnrnpd*^{tm1Rjsc} mice (n=34, solid black), B6;129S6 wild-type and heterozygote mice (n=31, dotted black), 129S6-*Hnrnpd*^{tm1Rjsc} mice (n=21, solid blue), and 129S6 wild-type and heterozygote mice (n=24, dotted blue). “Skin lesions” were categorized as dermatitis beyond palpebral involvement, refer to (**e**–**i**). *P<0.0001.

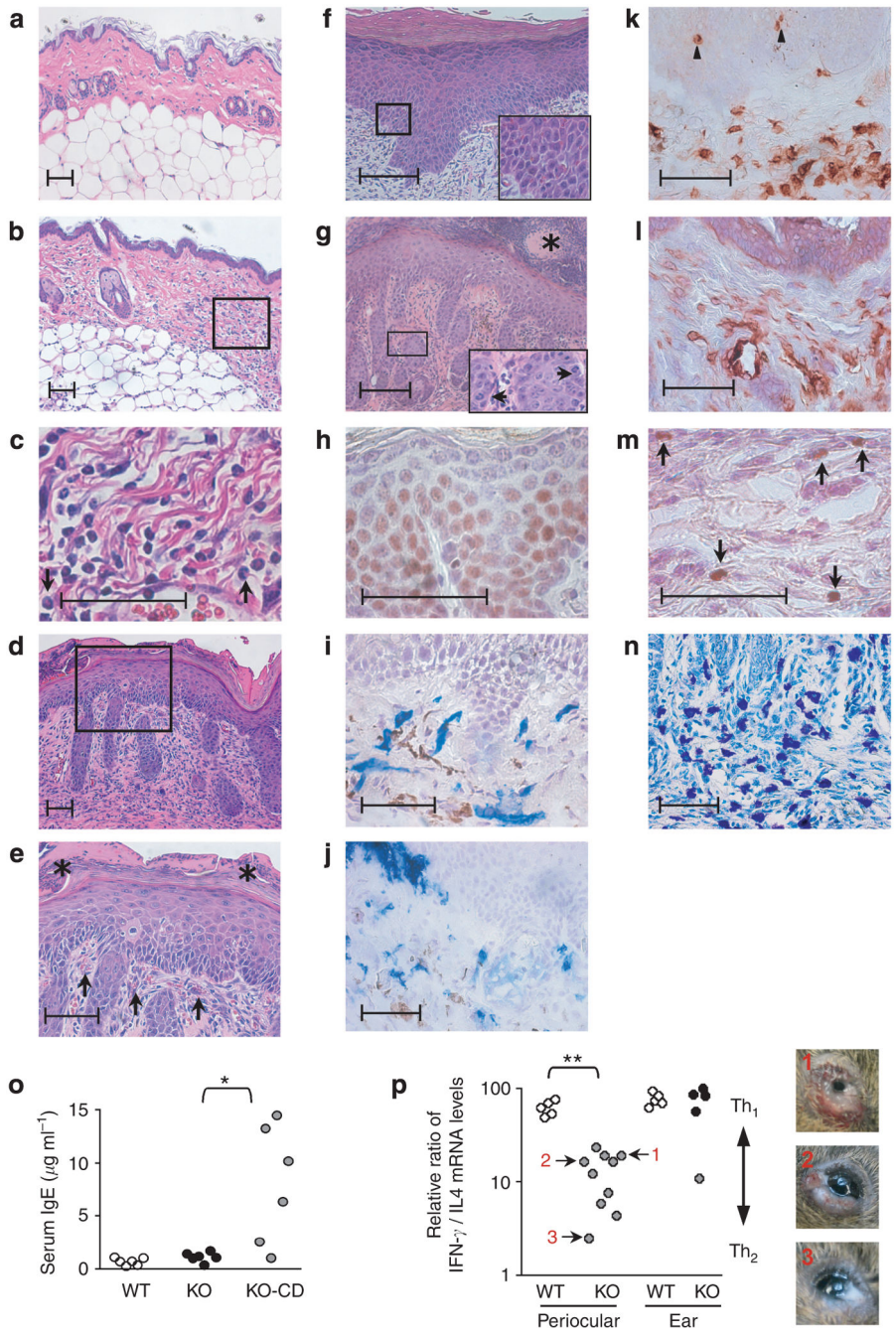

Figure 2. Histopathology of lesions

(**a**–**e**) Hematoxylin/eosin (H/E) staining of skin sections taken from the dorsum of the same 11-month-old *Hnrnpd*^{tm1Rjsc} mouse with chronic lesions at 2 cm from lesion (**a**), 1cm from lesion (**b**, **c**), and at the lesion (**d**, **e**). (**c**, **e**) are enlarged magnification of rectangle in (**b**, **d**), respectively. (**a**) Non-lesion skin in *Hnrnpd* ^{tm1Rjsc} mice normally consists of one or two epidermal layers overlaying a noninflammed dermis. (**b**, **c**) Skin neighboring lesion shows (**c**) large infiltration of neutrophils, mononuclear cells, and a few eosinophils (arrows) without discernable epidermal changes. (**d**, **e**) Chronic lesions show marked epidermal

acanthosis with spongiosis, hyperkeratosis, parakeratosis, prominenet dermal infiltrate, and neocascularization. Arrows in (**e**) highlight capillaries near dermoepidermal border. (**f**, **g**) Representative H/E sections from other chronic lesions from ear (**f**) and face (**g**) of 10-month-old *Hnrnpd* ^{tm1Rjsc} mice showing similar changes. Insert in (**f**) shows an example of spongiosis, and in (**g**) shows an example of leukocyte infiltrate in the epidermis (arrows). (**e**, **g**) Neutrophil aggregates composed of pykotic neutrophilic debris, eosinophilic serum, and occasional staphylococcal colonies (*) located above parakeratotic stratum corneum are seen in severe chronic lesions. (**h**) Acute lesions demonstrate strong PY-Stat3 staining (brown). (**i**–**l**) Immunostaining of a chronic lesion from facial skin demonstrating (**i**) neovascularization ($CD31^+$, blue), (**j**) infiltrate of dermal and epidermal abscess of neutrophils ($Gr\text{-}1^+$, blue), (**k**) dermal and epidermal (arrowheads) T cells ($CD3^+$, brown), and (**l**) dermal macrophages ($F4/80^+$, brown). (**m**) Staining by 3,3′-diaminobenidine plus nickel chloride (DAB-Ni) demonstrates the presence of eosinophils (arrows) in dermis of chronic lesions. (**n**) Toluidine blue staining demonstrates large number of dermal mast cells in chronic lesions. Scale bar=0.1mm. (**o**) Serum IgE levels were tested by ELISA from 8- to 12-month-old wild-type mice (white), and *Hnrnpd* ^{tm1Rjsc} mice free of lesions (black) or with chronic dermatitis (CD, gray). (**p**) Ratio of IFN-γ mRNA levels relative to IL4 mRNA levels in periocular and ear biopsies from *Hnrnpd* ^{tm1Rjsc} with dermatitis and wild-type controls. Biopsies taken from sites with overt dermatitis or blepharitis are shaded in gray. Each circle represents values from an independent biopsy. Periocular biopsies were taken from both eyes in *Hnrnpd* ^{tm1Rjsc} mice and left eye in wild-type littermates. Five mice were surveyed for each genotype. Numbers in red on the graph and corresponding images (right) represent examples of lesions surveyed. *P<0.02, **P<0.001.

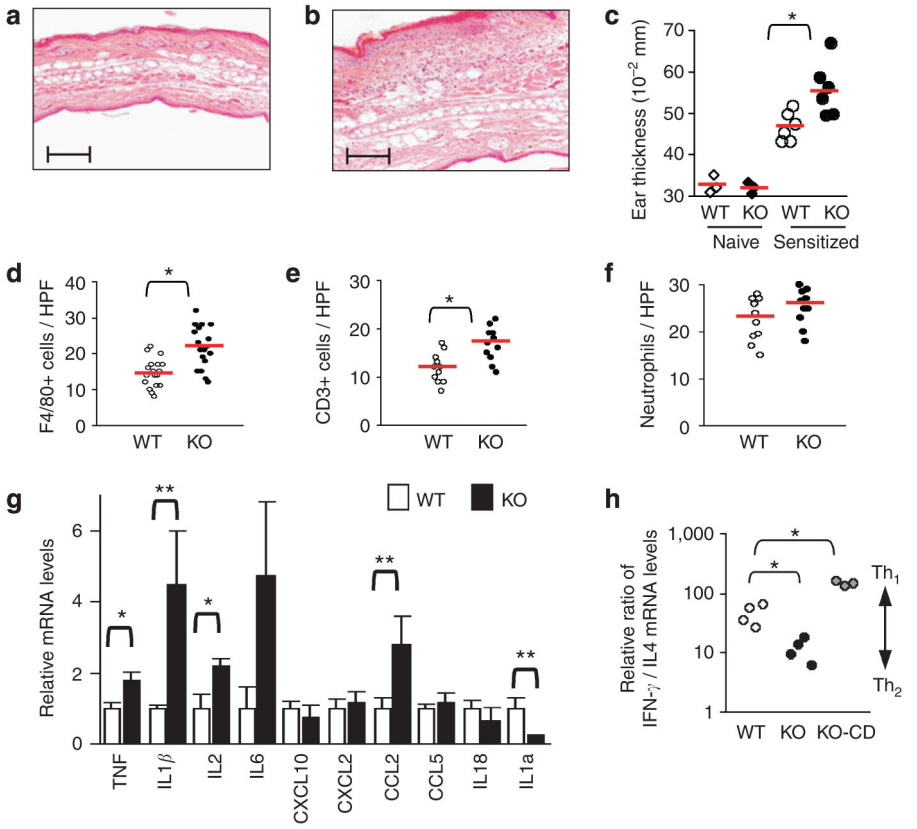

Figure 3. Increased CHS in *Hnrnpd*^{tm1Rjsc} mice

(**a**, **b**) H/E-stained section of ears collected 24 hours post-DNFB elicitation from DNFB-sensitized (**a**) wild-type (WT) and (**b**) *Hnrnpd*^{tm1Rjsc} (KO) littermates. Scale bar=0.2 mm. (**c**) Ear thickness 24 hours post-DNFB elicitation in naïve or DNFB-sensitized WT and KO littermates. Each diamond or circle represents measurements of one mouse and red bar represents the mean in each group. (**d**, **e**) Counts of the number of (**d**) macrophages (F4/80^{+}), (**e**) T cells (CD3^{+}), and (**f**) neutrophils per high-power field (HPF, ×400 magnification) in DNFB-elicited ears from DNFB-sensitized control WT and KO littermates. (**g**) Relative mRNA levels in ears of DNFB-sensitized wild-type mice (white bars) and *Hnrnpd* ^{tm1Rjsc} littermates (black bars) 24 hours post-DNFB elicitation as determined by qRT-PCR. Each bar represents mean±SD of six mice. (**h**) Ratio of IFN-γ mRNA levels relative to IL4 mRNA levels in ears of DNFB-sensitized wild-type mice (white), *Hnrnpd*^{tm1Rjsc} littermates (black), and *Hnrnpd*^{tm1Rjsc} mice with chronic dermatitis (CD, gray) 24 hours post-DNFB elicitation. *P<0.05, **P<0.01.

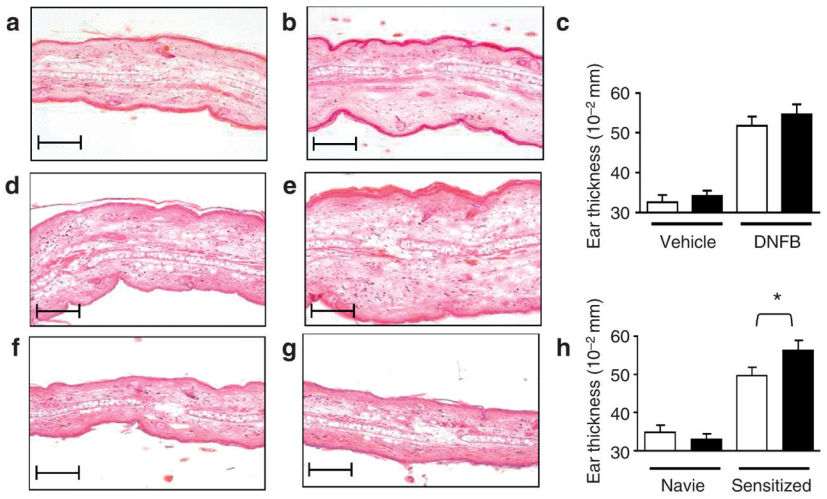

Figure 4. CHS in naïve mice adoptively transferred with DNFB-sensitized T cells

(**a**–**c**) *Hnrnpd*^{tm1Rjsc} mice and wild-type littermates were sensitized with 0.5% DNFB and T cells from draining lymph nodes were harvested 5 days later. Pooled T cells were injected into the base of the ear of naïve wild-type mice and subsequently ears were challenged with 0.2% DNFB. (**a**, **b**) Representative H/E-stained section of ears collected 24 hours post-DNFB elicitation from the same mouse. T cells from DNFB-sensitized wild-type mice were injected into the left ear (**a**) and T cells from DNFB-sensitized *Hnrnpd*^{tm1Rjsc} littermates were injected to the right ear (**b**). (**c**) Ear thickness 24 hours after elicitation with vehicle alone (vehicle, *n*=2) or DNFB (*n*=4) in naïve wild-type mice injected with T cells from DNFB-sensitized wild-type mice (white bar) and *Hnrnpd*^{tm1Rjsc} littermates (black bar). (**d**–**h**) Wild-type mice were sensitized with 0.5% DNFB and T cells from draining lymph nodes were harvested 5 days later. Pooled T cells were injected into the base of the right ear of naïve *Hnrnpd*^{tm1Rjsc} mice and littermate wild-type mice and ears were subsequently challenged with 0.2% DNFB. As a control, T cells from naïve wild-type mice were injected into the left ears of recipient mice before challenge. Representative H/E-stained section from (**d**) right (receiving sensitized T cells; ‘sensitized,’ white bar in (**h**)) and (**f**) left (receiving naïve T cells; ‘naïve,’ white bar in (**h**)) ears of a wild-type mouse and from (**e**) right (‘sensitized,’ black bar in (**h**)) and (**g**) left (‘naïve,’ black bar in (**h**)) ears of a *Hnrnpd*^{tm1Rjs} littermate 24 hours post-DNFB elicitation. (**h**) Plot of ear thickness 24 hours post-DNFB elicitation. Scale bar=0.2 mm. Histograms represent mean±SD of four mice. *P<0.05.

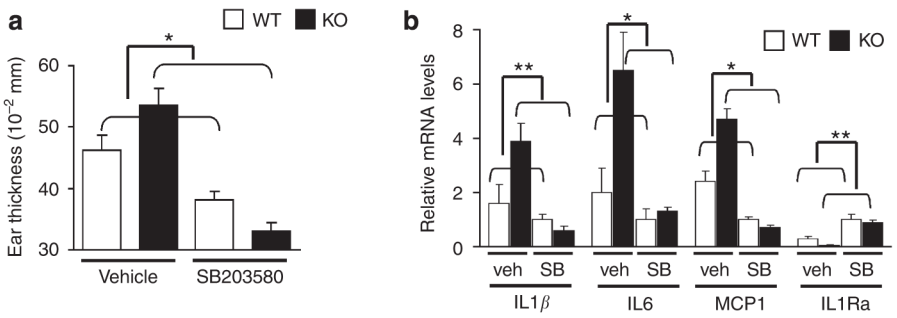

Figure 5. p38 MAPK inhibition blocks enhanced CHS in *Hnrnpd*^{tm1Rjs} mice

(**a**) Ear thickness 24 hours post-DNFB elicitation from wild-type (WT; white bar) and *Hnrnpd*^{tm1Rjsc} (KO; black bar) littermates that were either pretreated with vehicle or p38 MAPK inhibitor, SB203580, 30 minutes before elicitation. (**b**) Relative mRNA levels as determined by qRT-PCR 24 hours post-DNFB elicitation in ears from WT and KO littermates that were either pretreated with vehicle (veh) or SB203580 (SB) 30 minutes before elicitation. Histograms represent mean±SD of three mice. The change between vehicle and inhibitor for each mouse was determined. Those differences were compared between KO and WT groups. *P<0.05, **P<0.01.

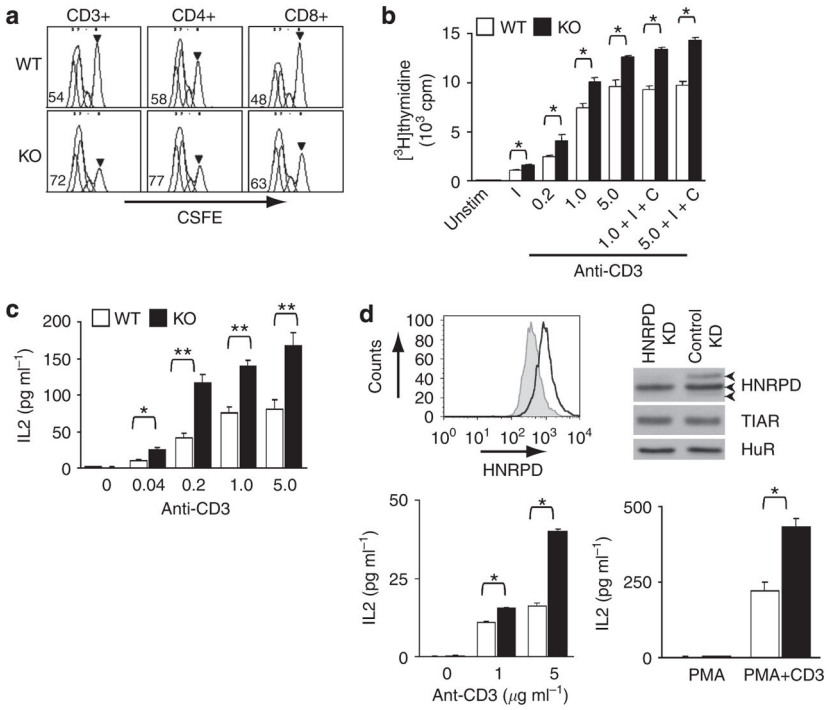

Figure 6. *Hnrnpd*-deficent T cells are hyperproliferative

(**a**) Analysis of cell division by CSFE labeling. Lymph node cells from 4-month-old *Hnrnpd* ^{tm1Rjs} (KO) and wild-type (WT) mice were labeled with CSFE and were left either unstimulated or stimulated with titrating concentrations of antibody to CD3 for 72 hours. Cells were stained with antibodies to CD3, CD4, and CD8 and analyzed by flow cytometry. Data shown are from $CD3^+$, $CD4^+$, and $CD8^+$ cells stimulated with 5 μgml^{-1} of anti-CD3. Peaks indicate successive divisions reflecting the dilution of CSFE with each division. Arrowhead indicates peak corresponding to the population of nondividing T cells. Numbers indicate the percentage of cells that have entered at least two rounds of cell division. (**b**) TCR-induced [^{3}H]thymidine incorporation. Splenic $CD4^+$ isolated T cells from 4-month-old wild-type (white bar) and *Hnrnpd* ^{tm1Rjsc} (black bar) littermates were left unstimulated (unstim) or were stimulated with antibody to CD3 (concentrations, μgml^{-1}, horizontal axis) with or without IL2 (I, 100 U) and antibody to CD28 (C, 1 μgml^{-1}) for 48 hours. [^{3}H]thymidine incorporation is presented as mean±SD of triplicate wells. (**c**) IL2 ELISA. Splenocytes from 4-month-old wild-type (white) and *Hnrnpd* ^{tm1Rjsc} (black) littermates were stimulated with titrating concentrations of antibody to CD3 for 24 hours. Supernatants were collected and IL2 levels were measured by ELISA. Data are presented as mean±SD of three independent experiments. (**d**) HNRNPD expression (top and left) by flow cytometry analysis in HNRNPD-knockdown (gray) and control-knockdown (bold) Jurkat T cells or by immunoblot analysis (top and right). In immunoblot analysis, staining with HNRNPD shows three bands (arrowheads) corresponding to the four isoforms of AUF1. Levels of other ARE-binding proteins, HuR and TIAR, are shown as controls. IL2 ELISA (bottom), control-knockdown (white), and HNRNPD-knockdown (black) Jurkat T cells were stimulated with antibody to CD3 (1 μml^{-1}) or phorbol myristate acetate (PMA; 10 ng ml^{-1}) for 24 hours and

secreted IL2 production was measured. Data are presented as mean±SD of two independent experiments. *P<0.05, **P<0.01.

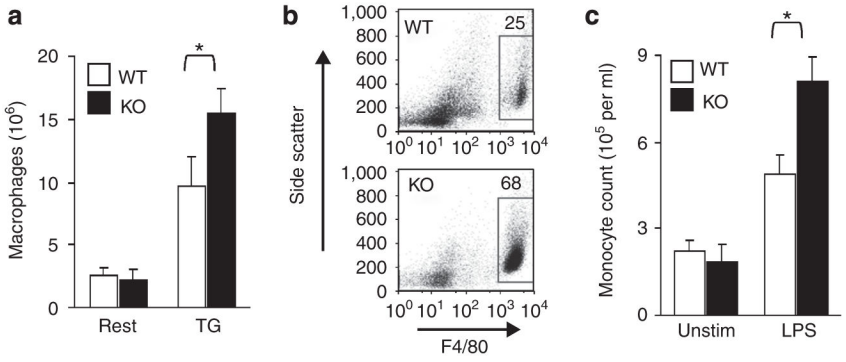

Figure 7. Increased macrophage recruitment to inflammatory stimuli in *Hnrnpd*^{tm1Rjsc} mice

(**a**) Thioglycollate elicitation in wild-type (white bars) and *Hnrnpd* ^{tm1Rjsc} littermates (black bars). Number of peritoneal macrophages (F4/80^{+} cells) in untreated (rest) and thioglycollate-injected (TG) mice. Each bar represents mean±SD of four mice. (**b**) Thioglycollate elicitation in 129S6-*Hnrnpd* ^{tm1Rjs} (KO) and wild-type littermates (WT). Representative flow cytometric analysis of peritoneal lavages performed 72 hours post-thioglycollate injection. Numbers indicate the percentage of F4/80^{+}-gated cells. (**c**) Peripheral blood monocyte counts post-lipopolysacchride (LPS) challenge in wild-type (white bars) and *Hnrnpd* ^{tm1Rjs} (black bars) littermates. Monocytes were counted before and 8 hours post-LPS challenge. Each bar represents mean±SD of three mice. **P*<0.05.

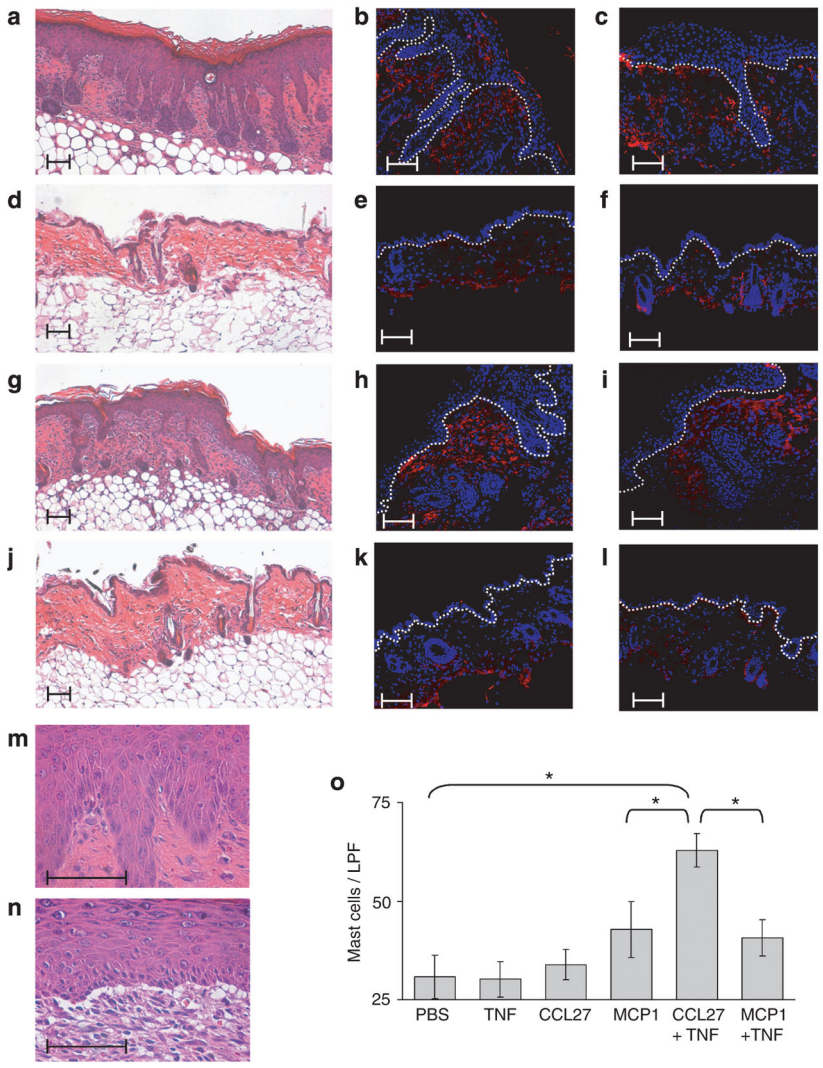

Figure 8. Subcutaneous injection of CCL27 and TNF in *Hnrnpd* ^{tm1Rjsc} mice results in eczematous dermatitis

(**a**–**f**) Representative skin samples from (**a**–**c**) *Hnrnpd* ^{tm1Rjsc} mice and (**d**–**f**) wild-type littermates 10 days after injection with CCL27 and TNF. (**g**–**l**) Representative skin samples from (**g**–**i**) *Hnrnpd* ^{tm1Rjsc} mice and (**j**–**l**) wild-type littermates 10 days after injection with MCP1. (**a**, **d**, **g** and **j**) H/E-stained, (**b**, **e**, **h** and **k**) T cells (CD3$^+$, red), and (**c**, **f**, **i** and **l**) macrophages (F4/80$^+$, red). Nuclei are counterstained blue. Dotted line indicates the dermoepidermal border. Enlarged magnification of lesions (**m**) induced by CCL27 and TNF injection and (**n**) induced by MCP1 and TNF to highlight differences in histological presentation. Changes in (**m**) resemble chronic spongiotic dermatitis, whereas changes in (**n**) more closely reflect interface dermatitis. Scale bar=0.1 mm. (**o**) Number of mast cells per low-power field (LPF, ×100 magnification) in toluidine-stained sections. Each bar represents mean±SD of counts from three mice. *P<0.05.